Performance analysis of load-strain models for circular columns confined with FRP composites

Composite Structures 94 (2012) 3115–3131: http://dx.doi.org/10.1016/j.compstruct.2012.04.036

PEDRO FAUSTINO MARQUES[1,2], CARLOS CHASTRE[2]

[1] Escola Superior de Tecnologia do Barreiro – Instituto Politécnico de Setúbal, Portugal, pedro.marques@estbarreiro.ips.pt

[2] Department of Civil Engineering, FCT/UNIC, Universidade Nova de Lisboa, Portugal, chastre@fct.unl.pt

Abstract

The use of FRP composites for the confinement of concrete has become an important aspect to consider on strengthening of concrete columns. It is important therefore that accurate modelling tools are available for the design of this strengthening system having into account, not only the peak values of load and strain, but also the complete stress-strain behaviour. A wide group of authors have proposed several models specific for FRP-confined concrete base either on theoretical assumptions (analysis oriented models – AOM) or on mathematical calibration from testing results (design oriented models – DOM). This article analyses 9 existing models for circular concrete columns in view of axially tested reinforced concrete columns confined with carbon reinforced polymers with three different diameters: 150; 250 and 400mm. The global shape of curves, peak compressive load, stress-strain relation, axial-to-lateral relation and dilation response were studied and compared to conclude which models' curves were closer to tests. Although a larger number of tests could give more accuracy to the study, the quantification of errors in face of the testing results was carried out for the most important parameters – ultimate load, strain and lateral stress – as well as for other curve parameters. Some models are accurate in predicting the peak load, though only few can accurately predict the load-strain and dilation behaviour.

Keywords: axial compression, analysis-oriented model, circular RC columns, confinement modelling, design-oriented model, dilation behaviour, FRP, passive confinement,

1. Introduction

The study of confining materials such as FRP for concrete columns has been the aim of several authors' research in order to enhance these elements' strength and ductility. Considering the importance of design calculations for new structures or the strengthening of existing ones, the modelling prediction of the performance of circular concrete columns subjected to axial compression is proposed by different authors as regards stress-strain behaviour.

The existing types of confining models are based on different premises and quantification of the properties of the materials and structural systems involved. Consequently, the approximation of these models' data against the real behaviour of tests is different for each model and with different influence on the several properties that characterize and quantify the performance of confined concrete columns. This evidence will be shown ahead in this article.

As in other structural systems, such as slabs and beams, the strengthening effect can be active or passive. In the specific case of actively-confined columns, stress state is laterally applied and externally controlled (Richart et al. 1928), being the lateral expansion restrained, while the axial stress increases. Several of the existing confining models are based on this principle. On the other hand, in passive confinement the confining stress of the strengthening is activated by the lateral expansion of the concrete core. In practice this is the behaviour of concrete cores confined with steel or FRP strips or jackets, though with distinct performance between these two materials expressed through the dilation properties and explained in section 4.4 (Mirmiran and Shahawy 1997; Samaan et al. 1998; Spoelstra and Monti 1999).

The existing confining models under axial compression may be divided into two groups (Lam and Teng 2003): (i) analysis-oriented models (AOM) and (ii) design-oriented models (DOM). In the first group most of these theoretical models are based on stress-strain curves of confined concrete obtained from active confinement curves by use of an incremental numerical process (Mander et al. 1988; Mirmiran and Shahawy 1997; Spoelstra and Monti 1999; Fam and Rizkalla 2001; Teng et al. 2007; Lee and Hegemier 2009). The second group includes models that are based on passive confinement and in which peak/ultimate stress and strain are first determined being then the non-linear behaviour is mathematically calibrated with experimental data (Karbhari and Gao 1997; Samaan et al. 1998; Toutanji 1999; Saafi et al. 1999; Lam and Teng 2003; Chastre and da Silva 2010).

The discussion around advantages or disadvantages between AOM and DOM in modelling the confinement under axial compression is still open, although some authors clearly consider AOM more accurate and DOM easier to implement due to their direct use in design calculations (Lam and Teng 2003; Jiang and Teng 2007).

Additionally, there is the fact that, in general, these models do not take into account the contribution of reinforcing steel hoops in concrete, whose influence varies as function of their quantity and spacing length as well as a function of quality of the confined concrete.

Given the necessity of understanding which models best fit the real behaviour of reinforced concrete (RC) columns confined with FRP jackets, including the contribution of transversal and longitudinal reinforcing steel, the present study aims to analyse 9 models of various authors – 4 AOM (Mirmiran and Shahawy 1997; Spoelstra and Monti 1999; Fam and Rizkalla 2001; Teng et al. 2007) and 5 DOM (Samaan et al. 1998; Toutanji 1999; Saafi et al. 1999; Toutanji revised [Matthys et al. 2006] and Chastre and da Silva 2010). All the models were implemented considering existing test results of reinforced concrete specimens 150, 250 and 400 mm diameter confined with CFRP Jackets. The modelling results are compared with test results in several parameters.

The experimental results herein used were carried out by Matthys (2000) and Chastre (2005) and beside different diameters the specimens had different CFRP Jackets and different number of layers. The analysis of modelling results compared with tests results is done in varied sides (stress-strain response, dilation properties, volumetric expansion, etc) with error quantification of several parameters for each model.

2. Test database

2.1 Tested columns

The experimental results, needed for the analysis of the several confining models, were obtained from the research group of the Universidade Nova de Lisboa and the open literature: 3 tests on CFRP-confined specimens with 150, 250 mm diameter (Chastre 2005) and 400 mm (Matthys 2000).

These circular cross-section specimens were of reinforced concrete with dimensions fairly considered as those of real existing construction columns. Fig. 1 shows the cross-section of the different columns whose experimental behaviour is to be compared with models' results. Table 1 presents the detailed constitution of the columns. The vertical reinforcement ratio is 1% for the 150 mm diameter column with 3 mm diameter stirrups spaced every 0.10 m, 1.4% for the 250 mm diameter column with 6 mm diameter hoops spaced every 0.15 m and 0.9% for the 400 mm diameter columns with 8 mm diameter hoops spaced every 0.14 m.

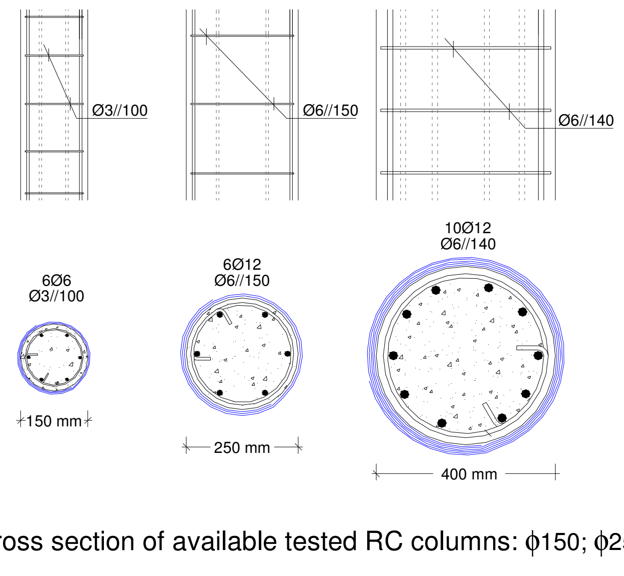

Fig. 1 – Cross section of available tested RC columns: ϕ150; ϕ250 and ϕ400

Table 1 – Constitution of available testes RC columns (Matthys 2000; Chastre 2005)

Column dimensions		Steel reinforcement		CFRP Confinement		
ϕ (mm)	Height (mm)	Longitudinal	Transverse	Sheet type	nº layers	t_{ply} (mm)
150	750	6ϕ6	ϕ3//0.10	A – Replark 30	2	0.167
250	750	6ϕ12	ϕ6//0.15	B – MBrace C1-30	2	0.176
400	2000	10ϕ12	ϕ8//0.14	C – S&P C240	5	0.117

Regarding the CFRP sheets, Replark 30 fibers applied with epotherm resin-L700S (here called type A) were used for 150 mm diameter specimen, MBrace C1-30 with MBrace Saturate resin (type B) for 250 mm diameter specimen and for 400 mm diameter C240 unidirectional sheet with Multipox T epoxy (Type C). For columns with 150 and 250 mm diameter, the overlap length of CFRP wraps was half of the perimeter of the column and for the 400 mm diameter the overlap length was of 200 mm.

2.2 Materials properties

Despite the available technical information from suppliers of some of the materials, tests were carried out in order to have more accurate results of the used samples. Table 2 summarizes the properties of all involved materials: concrete, steel reinforcement and CFRP sheets. The mean compressive results of unconfined concrete at 28 days age were: f_{c0}=38.0 MPa (ϕ150); f_{c0}=35.2 MPa (ϕ250); f_{c0}=34.3 MPa (ϕ400). For columns with 150 and 250 mm diameter the yield strength of steel reinforcement is 323 MPa for ϕ3, 391 MPa for ϕ6 and 458 MPa for ϕ12. For columns with 400 mm diameter the yield strength is 560 MPa for ϕ8 and 620 MPa for ϕ12. Tests on CFRP specimens resulted in: sheet type A, E_f=226GPa, f_{fu}=3339 MPa and ε_{cu}=1.44%; sheet type B, E_f=241 GPa, f_{fu}=3937 MPa and ε_{cu}=1.54%; sheet type C, E_f=198 GPa, f_{fu}=2356 MPa and ε_{cu}=1.19%.

Table 2 – Properties of tested materials (Matthys 2000; Chastre 2005)

Column	Concrete	Steel reinforcement		CFRP sheet			
ϕ (mm)	f_{c0} (MPa)	Diameter (mm)	Yield strength (MPa)	type	E_f (GPa)	f_{fu} (MPa)	ε_{fu} (%)
150	38.0	ϕ3	323	A	226	3339	1.44
		ϕ6	391				
250	35.2	ϕ12	451	B	241	3937	1.54
400	34.3	ϕ8	560	C	198	2356	1.19
		ϕ12	620				

2.3 Columns test results

In plain concrete columns confined with an external jacket the whole concrete is a core. During axial compression the load increases until the CFRP jacket reaches failure. In RC columns the behaviour is slightly different given the fact that the presence of steel hoops and longitudinal steel bars has a relevant contribution to columns' compression strength.

Depending on the contribution of confining hoops, there can still be some residual strength while buckling of longitudinal bars. As regards the available test data, the CFRP-confined specimens failed with sudden rupture of the jacket.

The results of the main parameters are shown in table 3 and the load-strain curves and dilation behaviour through-out testing are shown in figs. 2.

Due to the presence of steel reinforcement and hence diverse stress development during tests until failure, instead of stress-strain relation, fig. 2a shows the normalized load-strain relation where lateral strains ε_l are on the left side (tension – negative values) and axial strains ε_c on the right side (compressive – positive values). Also compared to load values, fig. 2b presents the normalized load-volumetric strain (N_c/N_0–ε_v) relation, in which positive value of ε_v represent volume contraction and negative values represent volume expansion. N_c is the axial compressive load and N_0 the maximum axial compressive load of unconfined concrete.

For a fair analysis it should be borne in mind that ϕ400 column, aside from having different CFRP sheet system, has also a different steel reinforcement grade.

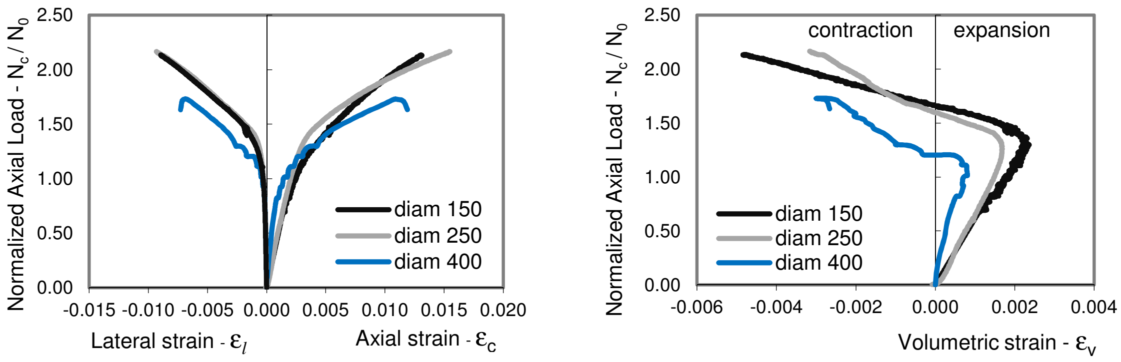

a) Axial load vs lateral and axial strains

b) Axial load vs volumetric strain

Fig. 2 – Load-strain relation of available tested CFRP-confined RC columns: ϕ150; ϕ250 and ϕ400 mm.

Table 3 –Tests results of CFRP-confined RC columns (Matthys 2000; Chastre 2005)

Column ϕ (mm)	N_0 (kN)	N_{cc} (kN)	N_{cc} / N_{co}	ε_{cc}	ε_{lu}
150	696.3	1485.7	2.13	0.0131	0.0090
250	1727.9	3741.6	2.17	0.0155	0.0093
400	4310.3	7460.0	2.03	0.0119	0.0073

N_0 = maximum axial load for unconfined concrete with steel reinforcement contribution: $f_{co} A_c + f_s A_s$

N_{cc} = maximum axial load for CFRP-confined concrete considering steel reinforcement contribution

ε_{cc} = axial strain at maximum axial load

ε_{lu} = lateral strain at failure of CFRP in hoop direction

3. Existing models for the confinement of circular cross-section concrete with FRP jackets

3.1 Introduction

In order to increase the compressive strength of concrete columns the use of confinement has been proved to be effective. Several models throughout the years have been developed to reflect concrete confinement and thus by this way estimating the gain in strength of a certain strengthening system. Some of the first models were developed for the confining effect of steel hoops in concrete elements (Mander et al. 1988) while others considered external steel jackets as strengthening material (Richart et al. 1928, 1929; Ahmad and Shah 1982) for circular-cross section columns.

With the possibility of using FRP in construction, either for strengthening or new construction, the previous models were apparently an obvious way to estimate confinement behaviour. However, due to the different properties of FRP, regarding steel, these models are less suitable in their present form when considering these materials (Matthys et al. 1999).

In view of the previous, some researchers have been developing different models based on extensive experimental data (Saadatmanesh et al. 1994; Howie and Karbhari 1995; Nanni and Bradford 1995; Picher et al. 1996; Mirmiran and Shahawy 1997; Matthys et al. 1999).

As mentioned before, confinement models are divided into two large groups – analysis-oriented models (AOM) and design-oriented models (DOM) – which have different principle approaches.

In AOM there is an explicit interaction between different materials (confined concrete and confining material – FRP, steel or others) and the calculation procedure assumes the compatibility between the lateral strain ε_l of actively-confined concrete with a constant confining pressure f_l equal to that given by the jacket. The stress-strain curve is generated by an incremental approach where curves with different active confinement levels generate a passive confinement curve (fig. 3a). In most cases the incremental procedure is iterative and hence not always of simple use for engineers.

In DOM, a specimen in concrete strengthened with FRP are considered as a "whole" reflecting the confinement behaviour based (calibrated) on experimental data, implying that active or passive confinement is already taken into account and it is represented by a two regions stress-strain relation (in some models bilinear), both axial and lateral (fig. 3b). These models are generally of simpler procedure in calculating, though in some cases the proposed equations are laborious.

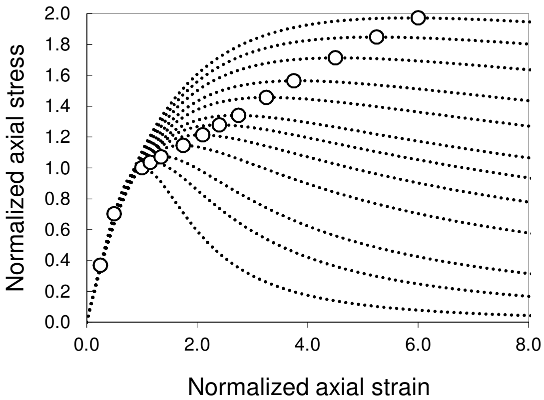

a) Passive confinement model (dots) generated by active confinement stress-strain curves (lines) (Mander et al. 1988) – AOM

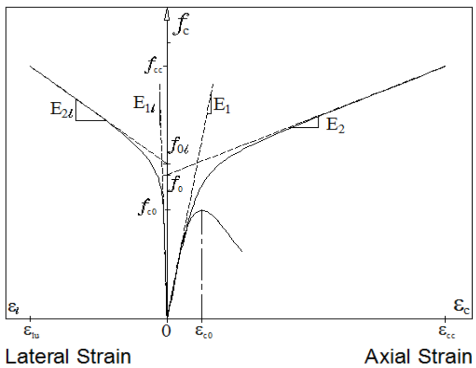

b) Two regions confinement model – DOM

Fig. 3 – Concept bases for confinement modelling

The group of confinement models based on the theory of fig. 3a analysed on this article includes: Mirmiran and Shahawy (1997); Spoelstra and Monti (1999); Fam and Rizkalla (2001) and Teng et. al. (2007). Those based on two regions confinement model (fig. 3b) are: Samaan et al. (1998); Toutanji (1999); Saafi et al. (1999); Toutanji revised (Matthys et al. 2006); Chastre and Silva (2010). All these models are for FRP-confined concrete columns.

3.2 Peak axial stress and corresponding strain

For unconfined concrete the ascending part of stress-strain curve is adopted in a reference code as Eurocode 2 (ENV 1992, 2004) considering a parabola as described in eq. (1):

$$\sigma_c = f_{co}\left(\frac{2\varepsilon_c}{\varepsilon_{co}} - \left(\frac{\varepsilon_c}{\varepsilon_{co}}\right)^2\right) \tag{1}$$

where σ_c the axial stress, ε_c the axial strain and, ε_{co} the axial strain at peak stress of concrete.

Nevertheless, this equation is not suited for representing the confinement behaviour of concrete since it cannot represent the gradual development of confinement (Lam and Teng, 2003a).

The basic concept behind the generalized modelling of peak stress of confined concrete was established by Richart, Brandtzaeg and Brown (1928) in which the failure strength of concrete confined by a hydrostatic fluid pressure (active confinement) takes the following form:

$$f_{cc} = f_{co} + k_1\, f_l \tag{2}$$

where f_{cc} is the maximum strength of confined concrete, f_{co} the maximum strength of unconfined concrete, f_l the lateral confining pressure and k_1 the confinement effectiveness coefficient.

Correspondingly, the axial strain ε_{cc} at which peak stress f_{cc} is reached, depends on the previous parameters and on the axial strain at maximum stress of unconfined concrete ε_{co} and takes the following form proposed by the same authors:

$$\varepsilon_{cc} = \varepsilon_{co} \left(1 + 5 k_1 \frac{f_l}{f_{co}} \right) \tag{3}$$

Equations (2) and (3) were used by Mander et al. (1988) who showed that the axial strain at maximum stress ε_{cc} can be expressed as a function of the strength of confined concrete f_{cc}:

$$\varepsilon_{cc} = \varepsilon_{co} \left[1 + 5 \left(\frac{f_{cc}}{f_{co}} - 1 \right) \right] \tag{4}$$

Another way to determine the peak axial stress is the one proposed by William and Warnke (1975) which is adopted by several analysis-oriented models for concrete confinement

$$f_{cc} = f_{co} \left(2.254 \sqrt{1 + 7.94 \frac{f_l}{f_{co}}} - 2 \frac{f_l}{f_{co}} - 1.254 \right) \tag{5}$$

Considering the purpose of studying FRP-confined concrete, the lateral pressure f_l at which the composite jacket fails is expressed as:

$$f_l = \frac{2\, t_f\, E_f}{D} \varepsilon_{h,rup} \tag{6}$$

Being t_f the sheet thickness, E_f the elastic modulus of the FRP composite, *D* the diameter of the column, $\varepsilon_{h,rup}$ the hoop strain at composite failure.

For the models herein studied Tables 4 and 5 show for AOM and DOM, respectively, the equations that each model uses to determine peak stress and the corresponding strain.

Table 4 – Peak stress and strain equations for AOM models

Analysis-oriented model	Peak stress	Eq. no. this article	Strain at peak stress	Eq. no. this article
Mirmiran and Shahawy (1997) Spoelstra and Monti (1999) Fam and Rizkalla (2001)	$f_{cc}=f_{co}\left(2.254\sqrt{1+7.94\frac{f_l}{f_{co}}}-2\frac{f_l}{f_{co}}-1.254\right)$ Based on William and Warnke (1975)	(5)	$\varepsilon_{cc} = \varepsilon_{co}\left[1+5\left(\frac{f_{cc}}{f_{co}}-1\right)\right]$ Based on Mander et al. (1988)	(6)
Teng et al. (2007)	$f_{cc} = f_{co} + 3.5 f_l$ based on Richart et al. (1928)	(7)	$\varepsilon_{cc} = \varepsilon_{co}\left[1+17.5\left(\frac{f_l}{f_{co}}\right)^{1.2}\right]$ from Eq. (6)	(8)

Table 5 – Peak stress and strain equations for DOM models

Design-oriented model	Peak stress	Eq. no. this article	Strain at peak stress	Eq. no. this article
Samaan et al. (1998)	$f_{cc} = f_{co} + 6 f_l^{0.7}\ [MPa]$ based on Richart et al. (1928)	(9)	$\varepsilon_{cc} = \frac{f_{cc} - f_0}{E_2}$	(10)
Toutanji (1999)	$f_{cc} = f_{co}\left[1+3.5\left(\frac{f_l}{f_{co}}\right)^{0.85}\right]$ based on Richart et al. (1928)	(11)	$\varepsilon_{cc} = \varepsilon_{co}\left[1+(310.87\varepsilon_{lu}+1.9)\left(\frac{f_{cc}}{f_{co}}\right)^{0.85}\right]$ calibrated based on Mander et al. (1988)	(12)

Saafi et al. (1999)	$f_{cc} = f_{co}\left[1+2.2\left(\frac{f_l}{f_{co}}\right)^{0.84}\right]$ based on Richart et al. (1928)	(13)	$\varepsilon_{cc} = \varepsilon_{co}\left[1+(537\varepsilon_{lu}+2.6)\left(\frac{f_{cc}}{f_{co}}-1\right)\right]$ calibrated based on Mander et al. (1988)	(14)
Toutanji revised (2006)	$f_{cc} = f_{co}\left[1+2.3\left(\frac{f_l}{f_{co}}\right)^{0.85}\right]$ Calibrated based on Toutanji (1999)	(15)	$\varepsilon_{cc} = \varepsilon_{co}\left[1+(537\varepsilon_{lu}^{*}+2.6)\left(\frac{f_{cc}}{f_{co}}-1\right)\right]$ 2nd region - $\varepsilon_{lu}^{*} = 0.6\,\varepsilon_{fu}$	(16)
Chastre and Silva (2010)	$f_{cc} = f_D + 5.29 f_l$ based on Richart et al. (1928)	(17)	$\varepsilon_{cc} = 17.65\,\varepsilon_{co}\left(\frac{f_l}{f_D}\right)^{0.7}$	(18)
			f_l obtained from $\varepsilon_{lu} = 0.6\,\varepsilon_{fu}$	(18-1)

ε_{fu} = failure (ultimate) strain of the CFRP material
ε_{lu} = failure (ultimate) strain of the CFRP jacket in hoop direction
f_0 = intercept stress in Samaan et al.'s model (fig. 3b)
f_D = axial compressive strength of unconfined concrete accounting for the tested core slenderness $f_D = \left(\frac{1.5+(D/H)}{2}\right) f_{co}$

It can be seen that all the AOM base their Eqs. (6) and (8) in Richart et al.'s model modified by Mander et al. for the determination of strain at peak stress (Table 4). For the peak stress Teng et al.'s model uses Richart et al.'s equation modified by with their own testing data (Eq. 7). The remaining three AOM authors use William and Warnke's equation (5) to determine the peak stress.

As to DOM authors (Table 5), the peak stress was calibrated from experimental data using Richart et al's eq. (2) (Eqs. 9, 11, 13, 15, 17) where Matthys, Toutanji et al. (2006) propose a revised form (eq. 15) of the equation (13) proposed by Toutanji (1999). The strain at stress peak in Toutanji and Saafi et al's models are based on Mander et al's equation (4) and calibrated with tests results (Eq. 12 and 14). Toutanji revised model (2006) adopts the equation (14) proposed by Toutanji (1999) but for the 2nd region the strain values are multiplied by 0.6 (eq. 16). Samaan et al. have their own equation (10) while Chastre and Silva adopted equation (18) calibrated from the experimental tests (Chastre and Silva 2010).

3.3 Stress-strain relation

i) AOM models

Mirmiran and Shahawy (1997) were the first to apply a passive confinement model based on incremental approach of actively-confined curves to FRP-confined concrete. The axial stress-axial strain relation is based on Popovics (1973) (eqs. 19, 19-1) being the lateral strains obtained from their relation with axial strains through dilation, since for linear elastic materials such as FRP the confining pressure rises in order to contain dilation. Therefore, the model presents equations to determine the dilation curve based on the authors' own tests.

Spoelstra and Monti (1999) created a model that uses an incremental-iterative approach to calculate the stress–strain behaviour of the FRP-confined concrete. The stress-strain relation is also based on Popovics modified by Mander et al. (1988) and the lateral-to-axial relation based on Pantazopoulou and Mills (1995).

As the previous the model of Fam and Rizkalla (2001) is based on Popovics' model adapted by Mander at al. (1988) but for concrete cores confined by FRP tubes. Peak stress, corresponding strain and stress-strain relation are the same of the previous models (Tables 5 and 6) but with its own axial-to-lateral relationship based on Gardner (1969) results and thus creating an equation to quantify the variation of Poissons' ratio under constant lateral confining pressure.

The model of Teng et al. (2007) is also an AOM with incremental-iterative approach but differs from the former as regards the equations to determine the peak stress and its corresponding strain and the lateral-to-axial relationship. The authors use Richart et al's equations calibrated with their research group testing results and propose a general equation to represent the dilation properties (eq. (26)) that is applicable to unconfined, actively confined and FRP-confined concrete.

Table 6 – Stress-strain relation of each model

Models	Stress-strain relation	Eq. no. this article
Mirmiran & Shahawy (1997) Spoelstra & Monti (1999) Fam & Rizkalla (2001) Teng et al. (2007)	$f_c = \dfrac{(\varepsilon_c / \varepsilon_{cc}) r}{r - 1 + (\varepsilon_c / \varepsilon_{cc})^r}$ $\quad r = \dfrac{E_c}{E_c - (f_{cc} / \varepsilon_{cc})}$ Popovics (1973) and Mander et al. (1988)	(19) and (19-1)
Toutanji (1999) Saafi et al. (1999) Toutanji revised (2006)	$f_c(\varepsilon_c) = \dfrac{E_1\ \varepsilon_c}{1 + \left[\dfrac{E_1}{f_a} - \dfrac{2}{\varepsilon_{1c}} + \dfrac{E_2 E_1 \varepsilon_{1c}}{f_a^2}\right]\varepsilon_c + \left[\dfrac{1}{\varepsilon_{1c}^2} - \dfrac{E_2 E_1}{f_a^2}\right]\varepsilon_c^2}$	(20)
	$f_c(\varepsilon_c) = \dfrac{E_{1l}\ \varepsilon}{1 + \left[\dfrac{E_{1l}}{f_a} - \dfrac{2}{\varepsilon_{1l}} + \dfrac{E_{2l} E_{1l} \varepsilon_{1l}}{f_a^2}\right]\varepsilon_l + \left[\dfrac{1}{\varepsilon_{1l}^2} - \dfrac{E_{2l} E_{1l}}{f_a^2}\right]\varepsilon_l^2}$ Toutanji (1999) based on Ahmad & Shah (1982) and Richart et al. (1929)	(21)
Samaan et al. (1998) Chastre & Silva (2010)	$f_c(\varepsilon_c) = \dfrac{(E_1 - E_2)\,\varepsilon_c}{\left[1 + \left(\dfrac{(E_1 - E_2)\,\varepsilon_c}{f_0}\right)^n\right]^{\frac{1}{n}}} + E_2\ \varepsilon_c$	(22)
	$f_c(\varepsilon_c) = \dfrac{(E_{1l} - E_{2l})\,\varepsilon_l}{\left[1 + \left(\dfrac{(E_{1l} - E_{2l})\,\varepsilon_l}{f_{0l}}\right)^{nl}\right]^{\frac{1}{nl}}} + E_{2l}\ \varepsilon_l$ Richard and Abbott (1975)	(23)

f_c = axial stress
f_a = axial stress at intersection point between the and second zones
ε_{1c} = axial strain at intersection point between the and second zones
ε_{1l} = lateral strain at intersection point between the and second zones
E_1, E_{1l} = 1st region slope for stress vs axial and lateral strains, respectively
E_2, E_{2l} = 2nd region slope for stress vs axial and lateral strains, respectively
n = shape factor for the axial stress – axial strain relation
n*l* = shape factor for the axial stress – lateral strain relation

ii) DOM models

Although incremental but with no need of iteration the models of Toutanji (1999) and Saafi et al. (1999) are DOM and based on the same approximation based on two equations for two region behaviour. The initial equation of Ahmad and Shah (1982) is used for the 1st region and Richart et al.'s equation (1929) for the 2nd region modified by Toutanji (1999) (fig. 3b, table 6). Toutanji's model was based on testing of concrete cylinders confined with FRP sheets while Saafi et al.'s model was based on testing of FRP confining tubes. Peak stress and corresponding strain equations are therefore different (Table 5). As for Toutanji revised model (2006), this is entirely based on the same author's model (1999) though considering for the 2nd region the failure strain in hoop direction corresponding to 60% of the ultimate strain of the CFRP material.

Samaan et al. (1998) proposed a design-oriented model – non-incremental – based on a correlation between the dilation rate of concrete and the hoop (lateral) stiffness of the restraining FRP sheet. The authors used a single equation by calibrating the four parameter stress-strain relation proposed by Richard and Abbott (1975) with a bilinear model configuration for the two distinct regions and the use shape parameter for the transition zone. This is directly related to the material properties of the confining FRP and the concrete core. The 2nd region is proportional to the stiffness of the confining jacket.

Chastre and Silva (2010) proposed a model for CFRP-confined concrete cylinders based on the same single equation of Richard and Abbott (1975) and calibrated with tests (Eq. 22) in which the both stress-axial strain and stress-lateral-strain relationships are of bilinear type with a shape factor. In the axial stress-axial strain curve, the slope of the 1st region is considered identical to the one of the plain concrete, as the FRP jacket has a passive behaviour and is only activated for a level of lateral deformation similar to the maximum stress of the non-confined concrete. The same type of equation is used for the axial stress-lateral strain relationship (Eq. 23).

Table 7 – Axial-to-lateral relation of each model

Models	Axial-to-axial relation	Eq. no. this article
Mirmiran & Shahawy (1997)	$\varepsilon_l = \mu\,\varepsilon_c$	(24)
	$\mu = \dfrac{\mu_0 - 2\mu_0\left(\dfrac{\varepsilon_c}{\varepsilon_{co}}\right) + \mu_u\left(\dfrac{\mu_{max}-\mu_0}{\mu_{max}-\mu_u}\right)\left(\dfrac{\varepsilon_c}{\varepsilon_{co}}\right)^2}{1 - 2\left(\dfrac{\varepsilon_c}{\varepsilon_{co}}\right) + \left(\dfrac{\mu_{max}-\mu_0}{\mu_{max}-\mu_u}\right)\left(\dfrac{\varepsilon_c}{\varepsilon_{co}}\right)^2}$	(25)
Spoelstra & Monti (1999)	Implicit in the model using Pantazopoulou and Mills (1995)	-
Fam & Rizkalla (2001)	Implicit in the model	-
Teng et al. (2007)	$\dfrac{\varepsilon_c}{\varepsilon_{co}} = 0.85\left(1 + 8\dfrac{\sigma_l}{f_{co}}\right) \times \left\{\left[1 + 0.75\left(\dfrac{-\varepsilon_l}{\varepsilon_{co}}\right)\right]^{0.7} - \exp\left[-7\left(\dfrac{-\varepsilon_l}{\varepsilon_{co}}\right)\right]\right\}$	(26)
Samaan et al. (1998) Toutanji (1999) Saafi et al. (1999) Toutanji revised (2006) Chastre & Silva (2010)	Implicit by the bilinear both axial stress-lateral strain and axial stress-axial strain relationships	-

μ_0 = 0.2, initial dilation rate = Poisson's ratio of unconfined concrete

$\mu_{max} = -0.7611\,Ln\,(2E_j t_f / f_{co} D) + 4.0167$, peak dilation rate

$\mu_u = -0.1375\,Ln\,(2E_j t_f / f_{co} D) + 0.8646$, asymptotic dilation rate after decrease

ε_l = lateral strain

ε_c = axial strain

ε_{co} = peak axial strain for unconfined concrete

3.4 Dilation properties

As mentioned before the first confinement models were developed for steel-confined concrete columns. Due to distinct properties between steel and FRP, and whether the nature of confinement is active or passive, the understanding of the dilation behaviour of concrete is essential to the accuracy of proposed models.

According to current knowledge and from what experimental evidences show (fig. 2b) when confined concrete columns are axially loaded volumetric changes develop. As regards passive confinement, at a first stage the column shortens and a contraction of its volume takes place. This behaviour goes on until a certain point where the lateral pressure of the confining material is activated. The subsequent development may cause contraction or expansion (dilation), depending on the used confining material, with relevant effect on the axial stress-strain relation.

Considering actively-confined concrete, where the lateral confining pressure is kept constant, the volumetric response is not related with the axial stress-strain behaviour and its influence is only negligible over axial-lateral stress-strain relation (Grassl 2004, Mirmiran and Shahawy 1997).

In steel-(passively) confined concrete the lateral strain ε_l activates the axial stress f_c which increases until steel yields. However, it is likely that yield strength is reached long before the peak axial stress f_{cc} (Grassl 2004, Mirmiran and Shahawy 1997). Consequently the dilation behaviour does not affect f_{cc} and have little or negligible influence on axial strain at peak stress ε_{cc}, resembling what happens in active confinement (Grassl 2004).

Due to its linear elastic behaviour FRP-confined concrete with external passive jackets shows distinct dilation response compared to steel-confined concrete. This property allows the lateral strain and hence confining pressure to increase until failure of the FRP jacket is reached.

Accordingly, if the volumetric response is of expansion the passive confinement will be activated. The higher the volumetric expansion (dilation) the more actuated is the passive confinement and therefore the higher (stiffer) is the axial stress-strain relation, which can increase significantly the axial compressive strength.

4. Modelling results and discussion

4.1 General

The comparison of the models proposed by the authors herein presented was done in view of existing experimental results on CFRP-confined RC columns with different diameters. Despite being available in the open literature, with tests on specimens ranging from 75 to 400 mm diameter, most of the experimental programs were based on small-size cylinders – under 150 mm diameter (Silva and Chastre 2006).

Although the mentioned practical experience regarding the quantity of tests is unbalanced favouring small-size specimens, the analytical results of models is presented and compared with tests results of axially loaded columns with 150, 250 and 400 mm diameter.

It should be borne in mind that these models have unalike assumptions also in view of the different state of the art at the time they were developed. Therefore, the comparison does not limit itself to single parameter evaluation but the whole behaviour from unloaded sate until failure.

Regarding the basis of modelling, most models do not have into account that ultimate lateral hoop strain of the column does not equal the CFRP strain of the composite sheet as reported by Lam and Teng (2003) and Toutanji revised (2006): a) nonhomogeneous deformations due to internal concrete cracking and hence non-uniform stress distribution in the FRP jacket; b) additional stress concentration on FRP originated by buckling of longitudinal steel reinforcement; c) irregularities in the FRP composite (misalignment of fibres); d) multiaxial stress state due to bonding between concrete and the FRP which may introduce in the latter part of the axial loading. In the models of the present study this aspect is only accounted by Toutanji revised model (2006), Teng et al. (2007) and Chastre and Silva (2010) in which the ultimate hoop strain is taken as 60% of the composite strain failure – ε_{lu}=0.6 ε_f.

Given the fact that the tested specimens were RC columns, thus with longitudinal steel bars and transverse steel hoops, it is important to outline the fact that only the model of Chastre and Silva (2010) explicitly accounts for the presence of steel reinforcement. Nevertheless, for all the models the contribution of longitudinal steel was considered.

Figures 4 – 6 show the behaviour of tests and of the implemented models with different approaches for each analysed column diameter: 150, 250 and 400 mm. Each figure is a set of four graphs – a), b), c), d) – where load–strain and axial strain–lateral strain relations as well as dilation behaviour are presented. Tables 8 – 10 show the individual results of axial strain at maximum load ε_{cc}, maximum load N_{cc}, ultimate lateral stress f_l and corresponding errors as regards the tests results.

The option of presenting the relation between the axial load and both axial strain and lateral strain instead of stress-strain curves is due the presence of steel reinforcement in the concrete columns and the consequent difference in the properties and behaviour of concrete and steel

4.2 Load-strain relation and axial-to-lateral strain relation

For the 150 mm diameter column fig. 4a shows the load-strain curves of the experimental results and the modelling results are shown in Table 8 and figs. 7 – 9. As regards the shape of the load-axial strain curve, it appears that the models of Toutanji (1999), Toutanji revised (2006) and Chaste and Silva (2010) are those closer to the test curve, although the first is extended long beyond the test curve. Saafi et al. (1999) and Samaan et. al (1998) clearly show themselves more divergent. In the load-lateral strain relation (left side of the graph) Saafi et al. (1999), Samaan et al. (1998) and Teng et al. (2007) do not match the test curve. All the others seem aligned with the test curve though only Toutanji revised (2006) and Chastre and Silva (2010) models have their curve limits close to test result. The maximum load is overestimated by Toutanji 1999, Fam and Rizkalla 2001, Spoesltra and Monti 1999 and Mirmiran and Shahawy 1997, while it is underestimated by Teng et al. 2007. Saafi et al. 1999, Samaan et al. 1998 and Chastre and Silva 2010 have close results. For the axial strain, Toutanji revised, Teng et al. and Chastre and Silva seem close to test values (fig. 4b) while all others overestimate it. As to the relation between axial and lateral strains the closest curves are apparently those of Toutanji 1999, Saafi et al. 1999, Toutanji revised (2006), Teng et al. (2007) and Chastre and Silva (2010), being these last two the only models, among the ones analysed here, where the ultimate lateral strain is close the test result of ε_{lu}=0.009 m/m. The lateral strain directly links the lateral failure stress and therefore consistent differences between models (Table 8).

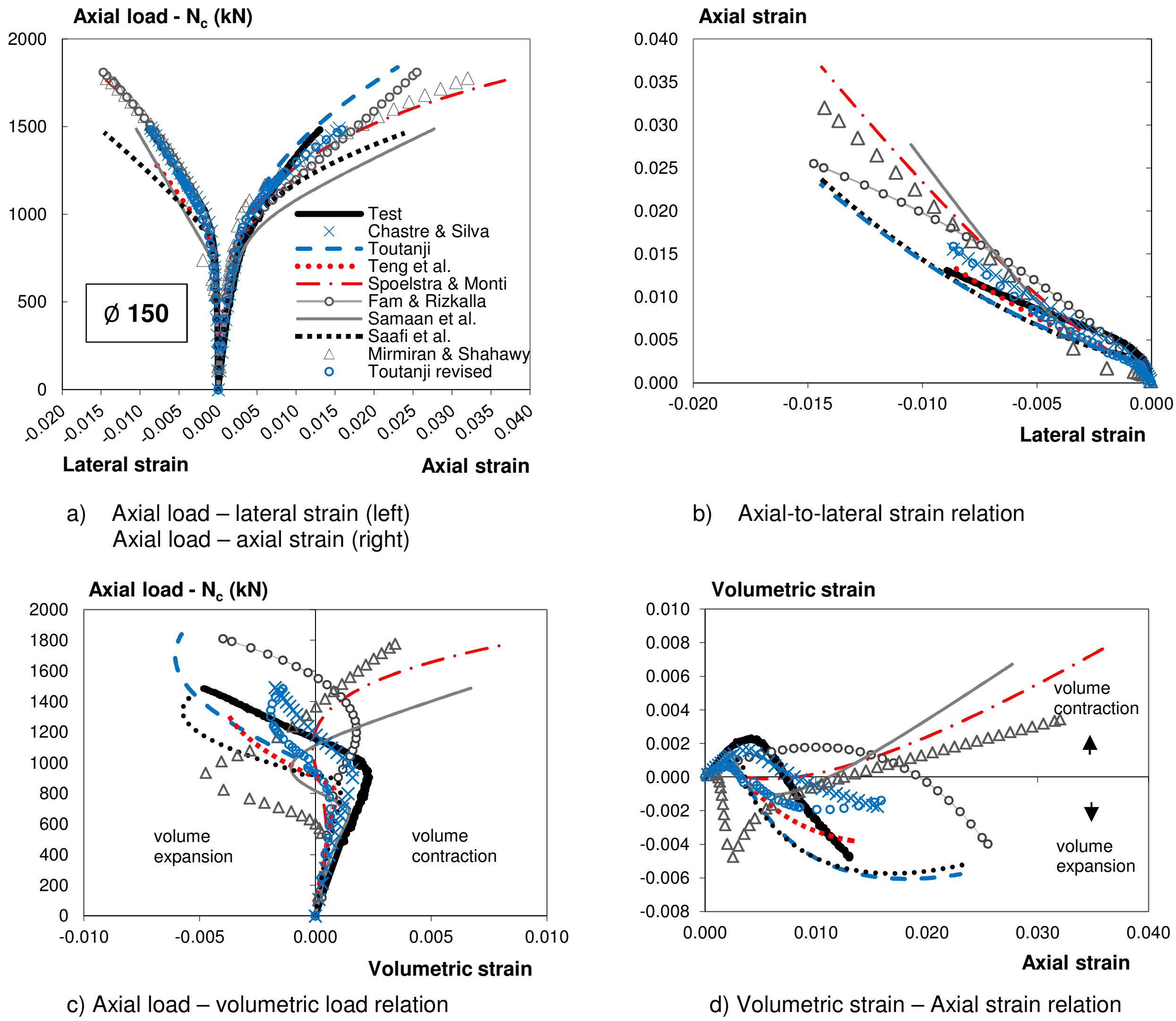

Fig. 4 – Test results vs models results: 150 mm diam. CFRP-confined RC column; 2 plies of t_f=0.167 mm

The results of the 250 mm diameter column are shown in figs. 5 and 7 – 9 and Table 9. The shape of load-strain curves show that Chastre and Silva (2010) model appears perfectly superposed to the test curve in both axial and lateral cases. For the load-axial strain relation, Toutanji revised curve (2006) show slightly underestimated values compared to the test curve, while Toutanji (1999) curve seems also close, though slightly overestimating the test values in the 2nd region of the curve and with load, axial and lateral strain values beyond the limits of test. All remaining curves present a lower shape development in terms of axial load until the ultimate axial strain of the test, though these models extend their curves outside the referred limit and some of them long beyond this limit (Mirmiran and Shahawy 1997 and Spoelstra and Monti 1999). For the load – lateral strain curve Saafi et al. (1999), Samaan et al. (1998) and Teng et al. (2007) show themselves more distant comparing with the others. As to the axial-to-lateral relation (fig. 5b) Chastre and Silva (2010) curve is visibly the closest to the test curve and with its end coincident with the test ultimate lateral strain ε_{lu}=0.0093 m/m.

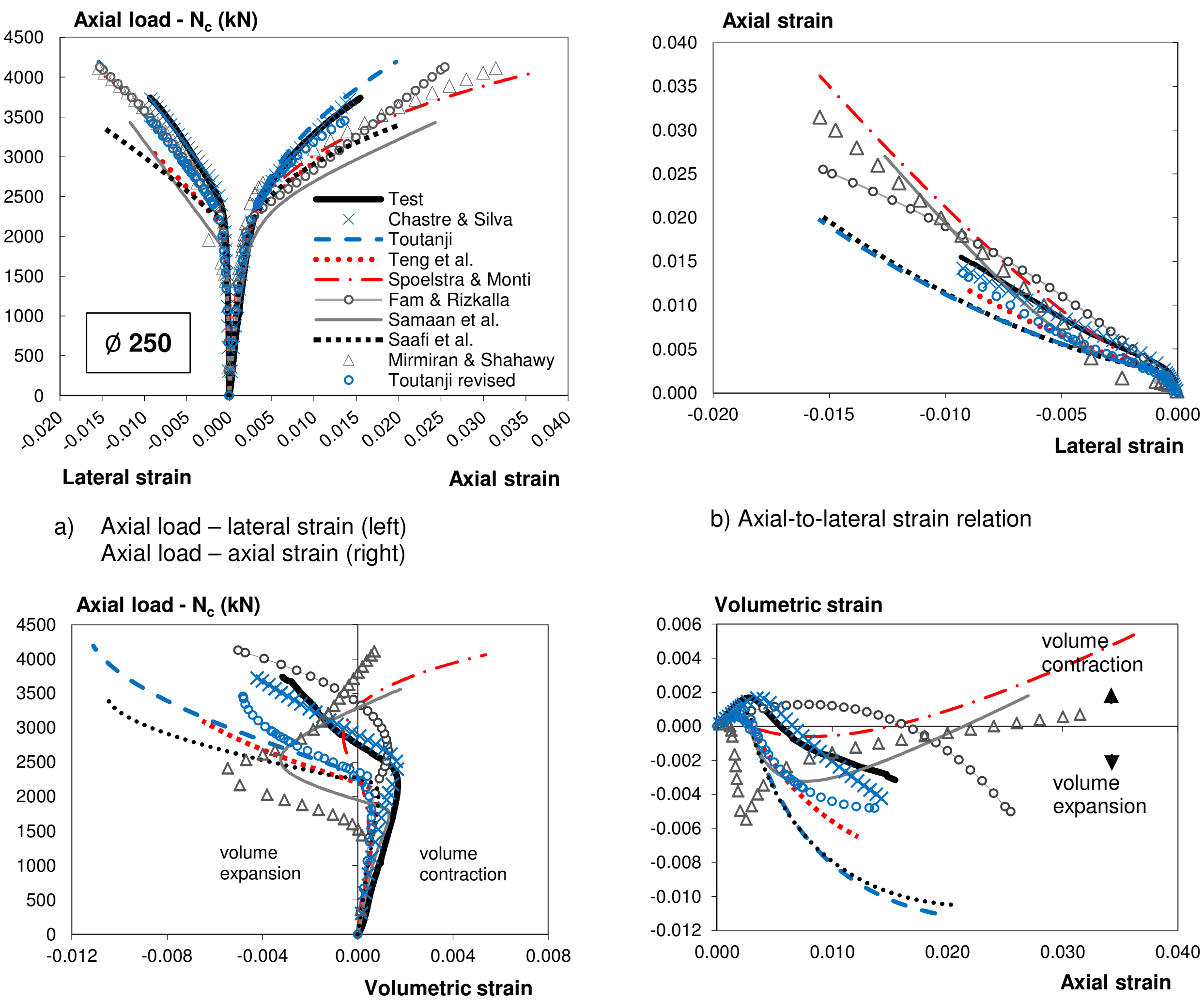

a) Axial load – lateral strain (left)
Axial load – axial strain (right)

b) Axial-to-lateral strain relation

c) Axial load – volumetric load relation

d) Volumetric strain – Axial strain relation

Fig. 5 – Test results vs models results: 250 mm diam. CFRP-confined RC column; 2 plies of t_f=0.176 mm

Following the same criteria analysis for the column with 400 mm diameter, the results are presented in fig. 6 and Table 10. Several models have a load-axial strain curve progression close the test. (Spoesltra and Monti 1999, Saafi et al. 1999, Teng et al. 2007 and Chastre and Silva 2010). Fam and Rizkalla (2001) is slightly under the test curve, while Mirmiran and Shahawy (1997) and Toutanji revised (2006) are slightly over it. Samaan et al. (1998) (under) and Toutanji (1999) (over) are considerably more distant. In the case of load-lateral strain curve, Samaan et al. (1998), Saafi et al. (1999) and Teng et al. (2007) present their curves progress below the test curve while the other are fairly superposed to this. Yet, again Mirmiran and Shahawy (1997), Spoelstra and Monti (1999), Toutanji (1999) and Fam and Rizkalla (2001) go beyond the failure lateral strain, while, except for the transition zone between the curve's 1st and 2nd regions, Toutanji revised (2006) and Chastre and Silva curves (2010) match the test curve, including the ultimate lateral strain. As to the axial-to-lateral relation Spoelstra and Monti's model (1999) appears to have the closest trend to test curve at the beginning, even though it moves away along the ending part of this one and it goes on past the limit of lateral strain of ε_{lu}=0.007 m/m. Chastre and Silva's model is the one that most fits the second half of the test curve.

It is interesting to verify that although Toutanji 1999 and Saafi et al's (1999) models have the same basis – the differences regard the calibration of FRP sheets and FRP tubes, respectively – they have distinct curves both load-axial strain and load-lateral strain (figs. 4a, 5a and 6a). However, concerning the axial-to-lateral relation their curves match perfectly between themselves.

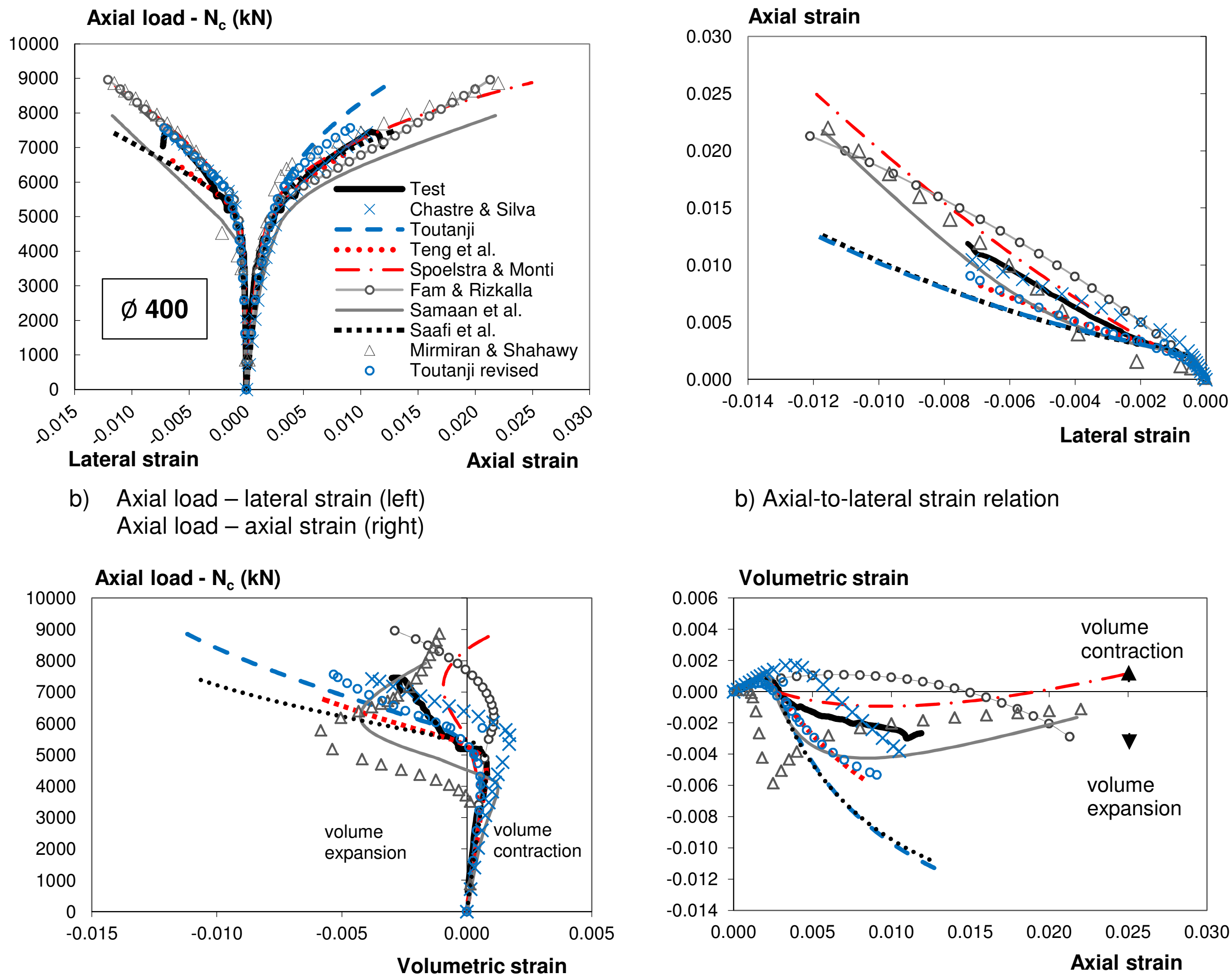

b) Axial load – lateral strain (left)
Axial load – axial strain (right)

b) Axial-to-lateral strain relation

c) Axial load – volumetric load relation

d) Volumetric strain – Axial strain relation

Fig. 6 – Test results vs models results: 400 mm diam. CFRP-confined RC column; 5 plies of t_f=0.117 mm

Table 8 – Modelling results for ϕ150 CFRP-confined column: N_{cc} ; ε_{cc}; f_l

Model	N_{cc} (kN)	Err (N_{cc}) (%)	ε_{cc}	Err (ε_{cc}) (%)	f_l (MPa)	f_l/f_{co}	Err (f_l/f_{co}) (%)
Test ϕ150	1486	-	0.0131	-	10.7	0.272	-
Chastre & Silva	1493	0.5	0.0155	18.5	9.1	0.270*	-0.6
Toutanji	1840	23.8	0.0230	75.5	14.5	0.368	35.5
Teng et al.	1327	-10.7	0.0135	2.7	8.7	0.221	-18.7
Spoelstra & Monti	1764	18.8	0.0368	180.3	14.5	0.368	35.4
Fam & Rizkalla	1799	21.1	0.0253	92.6	14.6	0.371	36.4
Samaan et al.	1487	0.1	0.0277	111.3	10.9	0.268	-1.3
Saafi et al.	1459	-1.8	0.0236	80.2	14.4	0.368	35.5
Mirmiran & Shahawy	1778	19.7	0.0320	144.0	14.4	0.365	34.3
Toutanji revised	1482	-0.2	0.0159	-21.1	14.5	0.368	35.4

* the ratio is in this case f_l/f_D (Table 5)

Table 9 – Modelling results for ϕ250 CFRP-confined column: N_{cc} ; ε_{cc}; f_l

Model	N_{cc} kN	Err (N_{cc}) %	ε_{cc}	Err (ε_{cc}) %	f_l MPa	f_l/f_{co}	Err (f_l/f_{co}) %

Test ϕ250	3742	-	0.0155	-	9.1	0.260	-
Chastre & Silva	3727	-0.4	0.0143	-8.0	7.0	0.217*	-16.5
Toutanji	4193	-12.1	0.0197	-27.1	10.4	0.297	-14.4
Teng et al.	3085	-17.5	0.0120	-22.2	6.3	0.178	-31.4
Spoelstra & Monti	4063	8.6	0.0362	133.5	10.5	0.297	14.3
Fam & Rizkalla	4128	10.3	0.0255	64.6	10.4	0.294	13.3
Samaan et al.	3561	-4.8	0.0270	74.4	9.3	0.264	1.4
Saafi et al.	3409	-8.9	0.0203	31.2	10.5	0.297	14.3
Mirmiran & Shahawy	4115	10.0	0.0315	103.4	10.5	0.297	14.4
Toutanji revised	3454	-7.7	0.0137	-11.7	10.5	0.297	14.3

Table 10 – Modelling results for ϕ400 CFRP-confined column: N_{cc} ; ε_{cc}; f_l

Model	N_{cc} (kN)	Err (N_{cc}) (%)	ε_{cc}	Err (ε_{cc}) (%)	f_l (MPa)	f_l / f_{co}	Err (f_l/f_{co}) (%)
Test ϕ400	7460	-	0.0119	-	6.8	0.199	-
Chastre & Silva	7428	-0.4	0.0105	-11.9	5.2	0.180*	-9.6
Toutanji	8757	17.4	0.0121	-1.0	6.7	0.194	-2.5
Teng et al.	6783	-9.1	0.0085	-28.6	4.1	0.121	-39.5
Spoelstra & Monti	8877	19.0	0.0249	109.6	6.9	0.201	0.9
Fam & Rizkalla	8965	20.2	0.0213	79.0	7.0	0.204	2.5
Samaan et al.	7493	0.4	0.0181	52.2	7.1	0.207	4.0
Saafi et al.	7457	0.0	0.0127	6.8	6.8	0.199	0.1
Mirmiran & Shahawy	8711	16.8	0.0205	72.3	6.3	0.183	-8.0
Toutanji revised	7473	0.2	0.0086	-27.4	6.7	0.194	-2.5

Having an overall observation of the three diameter results – figs. 4a, 5a and 6a – it is possible to realize that the load – lateral strain relation (left side) has more modelling curves matching the test curves than the load – axial strain relation (right side). Moreover, between the three sets of results, for each diameter, it is not possible to see or conclude any consistent evolution of the models in view of the diameter increase or decrease.

4.3 Error (Deviation) of N_{cc}, ε_{cc} and f_l/f_{co} for each model

It is possible from figs. 7 – 9 to have a global overview of the main parameters of each model for the three columns diameters: 150, 250 and 400 mm. The error in face of test results is quantified analysing the peak load N_{cc}, the axial strain at peak load ε_{cc}, and the confinement ratio f_l / f_{co}. The individual values of each model are presented in tables 8 – 10.

Figure 7 shows the deviation (in %) of the axial peak load. Chastre and Silva (2010) have a match in all three diameters followed by Samaan et al. (1998) with 0%, -5% and 0% and Toutanji revised (2006) with 0%, -8% and 0% for 150, 250 and 400 mm diameters, respectively. The remaining models present errors between 9% and 24%. However, although Samaan et al's model seems to be among those with less deviation as per N_{cc} results, figs. 4a, 5a and 6a clearly show that these authors' curves are the farthest from the tests curves. This indicates that the analysis of this sole parameter does not accurately represent the structural behaviour of axially confined columns.

As to the axial strain at peak load, the deviation is shown in the graph of fig. 8. The models with least deviation are Chastre and Silva (2010): 18%, -8%, -12%, Toutanji revised (2006): 21%, -12%, 7% and Teng et al. (2007): 3%, -22%, -29%. Toutanji 1999 and Saafi et al. 1999 give both a good approximation for 250 and 400 mm diameter columns (27%, 1%). Spoelstra and Monti (1999): 180%, 134%, 110% and Mirmiran and Shahawy (1997): 144%, 103%, 72% present values farther from tests results.

The results of the error of the confinement ratio are shown in fig. 9 and this factor is dependent of the failure lateral strain ε_{lu}. For the 150 mm diameter column Chastre and Silva's (2010) model has a little deviation of -1%, Teng et al. (2007) has -19%, while the remaining models, except for Samaan et al. (1998), have errors of approximately 35%. For the 250 and 400 mm diameter Teng et al.'s model presents deviations of -31% and -39%, respectively. Once more excluding Samaan et al. (1998), the results for the 250 mm diameter are between 13% and 17%. In the 400 mm diameter column, except for Teng et al.'s results, errors are between -10% and 4%. In this particular parameter Samaan et al. (1998) show the best fit for the three diameters with errors between -1% and 4%, even though the load–strain relation shows these model's curves as those farther from tests curves. This means that the confinement ratio alone has no sensitivity as regards the confinement model performance.

As it is, it appears that comparing modelling curves with tests curves, together with the previous parameters, is the most suited way of evaluating the performance of a confinement model.

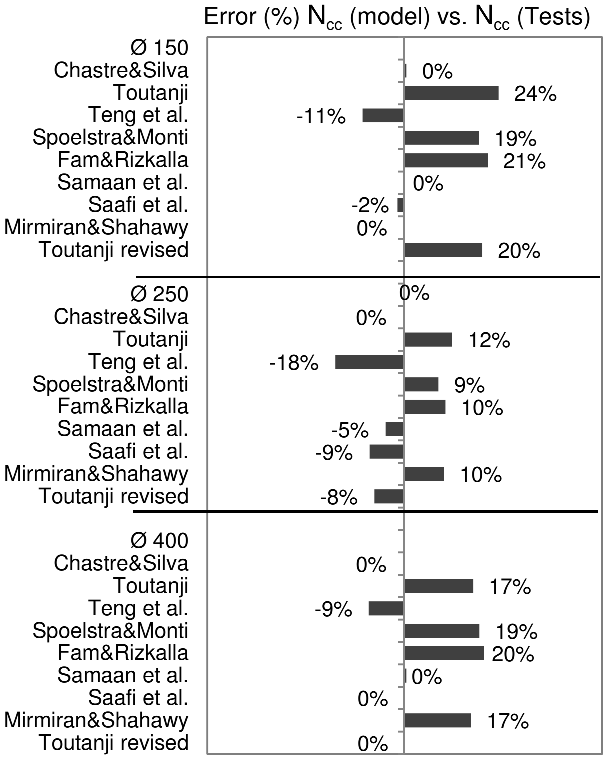

Fig. 7 – Error - models vs tests: Peak load N_{cc}.

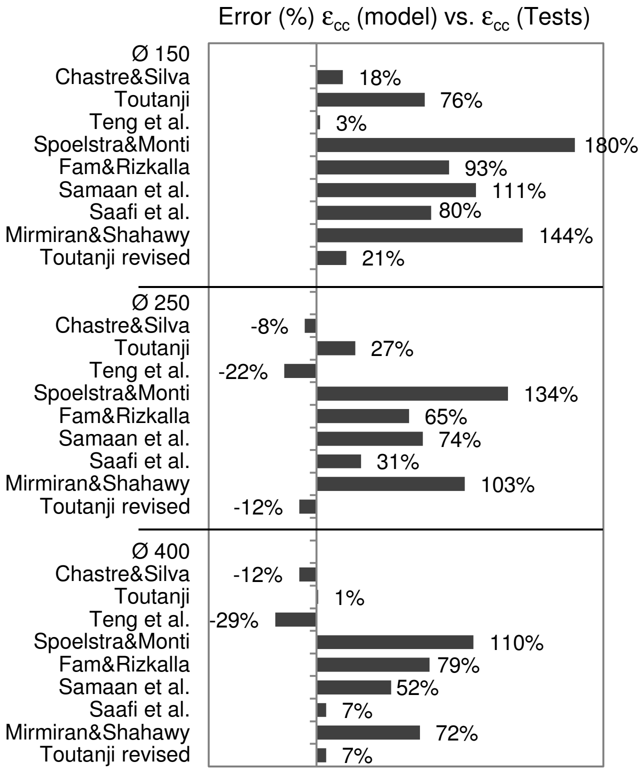

Fig. 8 – Error - models vs tests: Axial strain at peak load ε_{cc}.

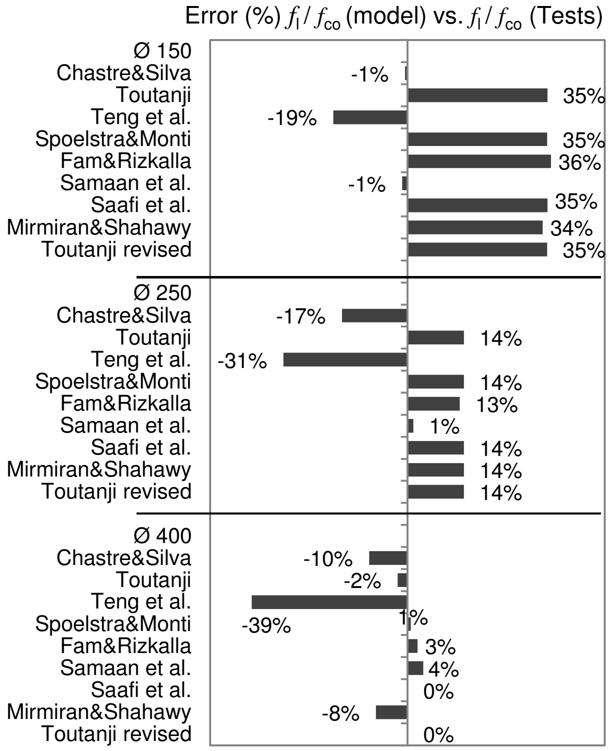

Fig. 9 – Error - models vs tests:
Confinement ratio at failure f_l / f_{co}.

4.4 Error (Deviation) of W_c, W_l and W_v for each model

Even considering the previous analysis, it is possible that the quantification of the observed curves is required for a complete approach to the analysis of all the models comparing with the tests results.

In view of this, additional parameters were created in order to observe the deviation between models and tests. Each of these parameters consists of the area underneath the curves to be analysed: W_c is the area of the axial load – axial strain curve; W_l is the area of the axial load – lateral strain curve; W_v is the area of the axial load – volumetric strain. In case of any physical meaning these parameters' units would be kN.m/m, the purpose is however to have an additional 'measure' of the deviation of each curve. Hence, these parameters are calculated according to the following expression:

$$W = \sum_{i=1}^{n} \left[\frac{1}{2} \left(y_i + y_{i+1} \right) \left(x_{i+1} - x_i \right) \right] \tag{27}$$

Where y is the ordinate of the graphic, x is the abscissa of the graphic, i is the index of summation and n is the upper bound of summation.

Herewith, tables 11-13 present the results of the mentioned parameters and figs. 10 – 12 show the error percentage of each model for all three tested columns: 150; 250 and 400 mm, respectively.

Table 11 – Parameters W_c, W_l, W_v – results for ϕ150 CFRP-confined column

Model	W_c (kNm/m)	Err (W_c) (%)	W_l (kNm/m)	Err (W_l) (%)	W_v (kNm/m)	Err (W_v) (%)
Test ϕ150	13		11		-8	
Chastre & Silva	17	-26.4	10	4.8	-3	58.2
Toutanji	13	4.6	10	7.8	-7	13.3
Teng et al.	14	-2.3	9	14.3	4	157.2
Spoelstra & Monti	51	-285.3	20	-85.0	12	258.0

Fam & Rizkalla	32	-139.2	20	-87.6	-8	0.6
Samaan et al.	31	-132.4	11	-6.7	8	208.4
Saafi et al.	11	15.6	9	18.1	-6	22.5
Mirmiran & Shahawy	44	-233.1	19	-76.5	7	191.4
Toutanji revised	17	-27.4	9	14.8	-2	74.3

Table 12 – Parameters W_c, W_l, W_v – results for ϕ250 CFRP-confined column

Model	W_c (kNm/m)	Err (W_c) (%)	W_l (kNm/m)	Err (W_l) (%)	W_v (kNm/m)	Err (W_v) (%)
Test ϕ250	43		28		-13	
Chastre & Silva	39	9.2	28	1.3	-16	-25.2
Toutanji	26	39.6	25	10.4	-24	-87.2
Teng et al.	29	32.9	23	16.8	-18	-37.0
Spoelstra & Monti	119	-174.6	49	-75.8	20	254.2
Fam & Rizkalla	76	-76.9	49	-73.6	-21	-62.6
Samaan et al.	74	-71.6	33	-18.4	8	159.1
Saafi et al.	55	-28.6	42	-50.9	-29	-125.6
Mirmiran & Shahawy	103	-139.2	48	-70.0	8	161.1
Toutanji revised	36	15.6	26	7.3	-15	-16.0

Table 13 – Parameters W_c, W_l, W_v – results for ϕ400 CFRP-confined column

Model	W_c (kNm/m)	Err (W_c) (%)	W_l (kNm/m)	Err (W_l) (%)	W_v (kNm/m)	Err (W_v) (%)
Test ϕ400	70		44		-18	
Chastre & Silva	58	17.7	45	0.4	-31	-70.0
Toutanji	38	45.3	44	1.7	-49	-165.9
Teng et al.	45	36.3	41	7.6	-37	-102.8
Spoelstra & Monti	179	-154.4	85	-90.7	10	154.5
Fam & Rizkalla	143	-102.9	86	-92.9	-28	-54.1
Samaan et al.	106	-51.1	60	-34.5	-13	29.1
Saafi et al.	75	-6.8	73	-65.3	-71	-290.2
Mirmiran & Shahawy	145	-106.5	71	-59.1	4	123.2
Toutanji revised	49	30.7	42	5.4	-35	-91.8

Concerning the load-axial strain relation and the associated parameter W_c (fig. 10), for the three diameters, Chastre and Silva (2010) (-26%, 9%, 18%), Toutanji (1999) (5%, 40%, 45%), Teng et al. (2007) (-2%, 33%, 36%), Saafi et al. (1999) (16%,-29%,-7%) and Toutanji revised (2006) (-27%, 15%, 74%) show closer values to the test curves than Spoelstra and Monti (1999), Fam and Rizkalla (2001), Samaan et al. (1998) and Mirmiran and Shahawy (1997) which range from -51% to -285%.

For the load–lateral strain relation and the parameter W_l (fig. 11) the closest models to the tests results are Chastre and Silva (2010), Toutanji (1999) and Teng et al. (2007) ranging from 0% to 17%. The remaining models show results between 18% and -93%.

The parameter W_v is the one with less direct approach when load-volumetric strain curves are observed once these represent different behaviour stages that may vary from volume contraction to volume expansion. In this case the signal is important and when negative it means that throughout the loading the volume expansion is prevailing in face of volume contraction. Table 13 and fig. 12 show that the results are highly scatter and that the model with less deviation for all diameters is Fam and Rizkalla's (2001) (2%, -54%, -63%) followed by Toutanji (1999) (13%) for 150 mm diameter, Toutanji revised (2006) (-16%) and Chastre and Silva (2010) (-25%) for 250 mm diameter and Samaan et al. (1998) (29%) for 400 diameter. Yet, figures 4c, 5c and 6c show that the model of Fam and Rizkalla (2001) seems less close to the tests curve when compared to Toutanji revised (2006) and Chastre and Silva (2010).

As it can be understood, despite the analysis of these parameters, similar values between two models do not mean that their curves' progression is close in terms of load or strain values or even that their shape is similar. The assessment should always cross the information of all parameters and the visual observation of graphs.

It is nevertheless important to quantify these parameters – W_c, W_l and W_v – to observe and explain the consistency of the columns behaviour with regard to different modelling approaches.

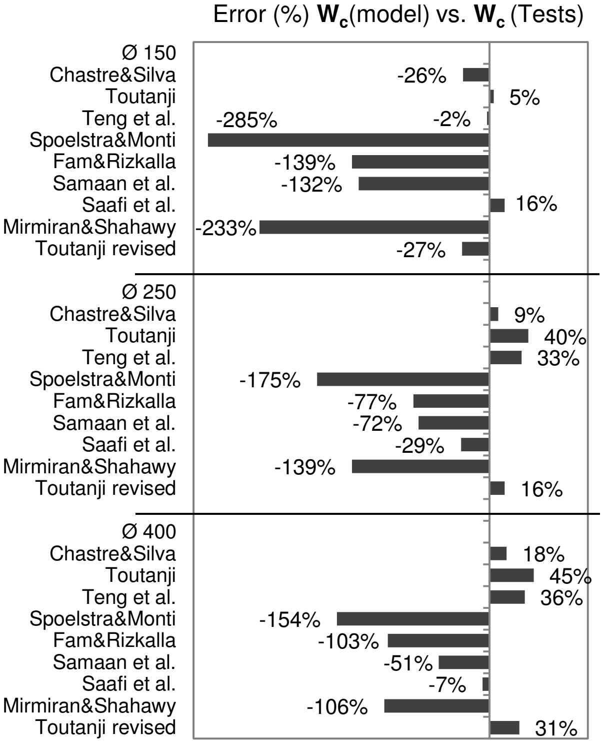

Fig. 10 – Error of models vs tests:
W_c – area of load vs axial strain relation (N_c x ε_c)

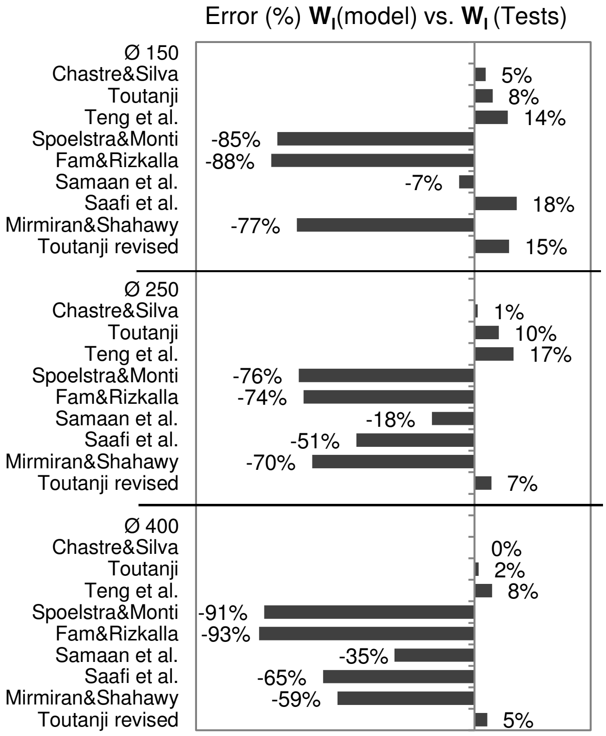

Fig. 11 – Error of models vs tests:
W_l – area of load vs lateral strain relation (N_c x ε_l)

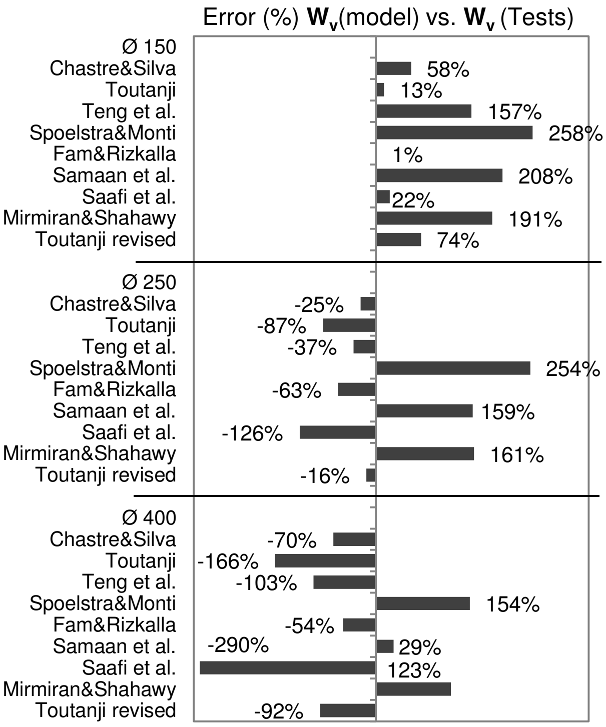

Fig. 12 – Error of models vs tests:
W_v – area of load vs volumetric strain relation (N_c x ε_v)

4.5 Dilation behaviour

The linear elastic behaviour of FRPs has a relevant effect on the development of deformations on concrete columns confined with this material. In view of what was described in section 3.4, FRPs provide a passive confinement when applied on concrete cores, which means that the composite material is only activated subjected to increasing concrete expansion, which means that lateral expansion FRP stress increases until failure. As a result, FRP performance distinguishes from active confinement, where external pressure is constant, and from steel confinement, where the lateral stress remains constant after steel yielding. Expansion has, thus, negligible influence stress-strain relation in both these cases.

Accordingly, the comprehension of the stress-strain (or load-strain) behaviour of FRP-confined concrete columns is evidently linked to its dilation behaviour. Progression of contraction and expansion in the course of load increase are governing as regards the activation of the confinement FRP sheet. Figs 4c, 4d, 5c, 5d, 6c and 6d present the results that express the dilation behaviour of tests and implemented models.

In the present study, with regard to AOM authors, Teng et al. model has a load – volumetric strain curve with shape similar to test, though with lesser contraction, with start of expansion at lower load and lesser expansion. Fam and Rizkalla (2001) have also a similar shape (contraction and then expansion) but at significant higher load. Mirmiran and Shahawy (1997) and Spoelstra and Monti (1999) present their models with contraction-expansion-contraction which differs from the test curve. In the volumetric strain – axial strain (figs. 4d–6d) relation the model of Mirmiran and Shahawy (1997) has a very different development comparing to the test curve and Fam an Rizkalla (2001) prolongs its contraction beyond the failure point. The main differences respecting this behaviour come from the axial-to-lateral relationship (Table 7).

For DOM it should be taken into consideration that the 2nd region slope depends on the FRP jacket stiffness which highly influences the axial-to-lateral relationship. Certainly, calibration influences the behaviour. Toutanji (1999) and Saafi et al. (1999) are based on the same model, with slight calibration differences, and have divergent development as regards load-volumetric strain but close curves in volumetric-axial strains relation, once the main calibration differences are related to peak stress and corresponding strain equations (Table 5) and not the axial-to-lateral relation.

The curve of Chastre and Silva (2010) maintains a shape with similar progress to the test curve for the three specimens, both for load – volumetric strain (figs. 4c–6c) and volumetric strain – axial strain (figs. 4d–6d) and it is one of the models closer to the test curve. Moreover, for 250 mm diameter column these authors' curve fairly matches the test curves, which is probably explained by the fact that these authors have calibrated their model with a large sample of 250 mm diameter specimens.

The models of Toutanji revised (2006) and Teng et al. (2007) seem to have the relation load-volumetric strain (fig. 6c) near to the test curve for 400 mm diameter, while for this relation Toutanji's model (1999) has a development close to the test curve but this model's curve is largely prolonged presenting considerably higher expansion.

4.6 Models with performance closer to tests' behaviour

Among the several models analysed, those proposed by Chastre and Silva (2010), Toutanji revised (2006) and Teng et al. 2007 seem to be closer to the tests results for the three studied diameters in all relations: load – axial and lateral strain; axial strain – lateral strain; load – volumetric strain and volumetric strain – axial strain.

Chastre and Silva's model have an almost perfect match for the three diameters for both load-strain relations (figs. 13a, 14a and 15a). Toutanji revised model presents curves close to test results though slightly underestimated for 150 and 400 mm diameter and with slight overestimate for 250 mm diameter. Teng et al's model is closer to the test results of the 400 mm diameter column as regards the shape of the curves. However, this model underestimates the axial load and even the values of axial strain for 150 and 400 mm diameter.

In the case of the lateral-to-axial relationship, Teng et al's model (2007) underestimates in general the axial strains as does Toutanji revised (2006) for 250 and 400 mm diameter. For 250 mm diameter Chastre and Silva's model (2010) has almost a perfect match, though with not such good performance for the columns with 150 mm and 400 mm diameter.

The dilation properties expressed through the relation between axial load and the volumetric strain (figs. 13c, 14c and 15c) as well as the relation between the volumetric and the axial strain show the difficulty of models in expressing this property which means that, except for Chastre and Silva (2010) with the 250 mm diameter column, none of the models herein presented could even be close to tests results. The main reason for this difference is the fact the volumetric strain depends on both axial and lateral strain and ($\varepsilon_v = \varepsilon_c + 2\varepsilon_l$) and in their relationship, which seems to be quite difficult to model in view of the experimental results.

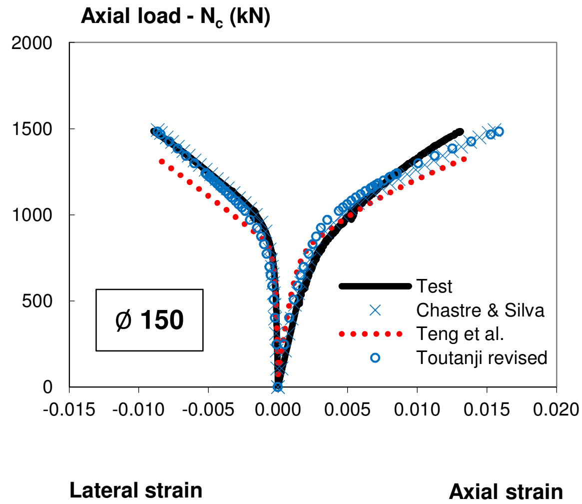

a) Axial load – lateral strain (left)
Axial load – axial strain (right)

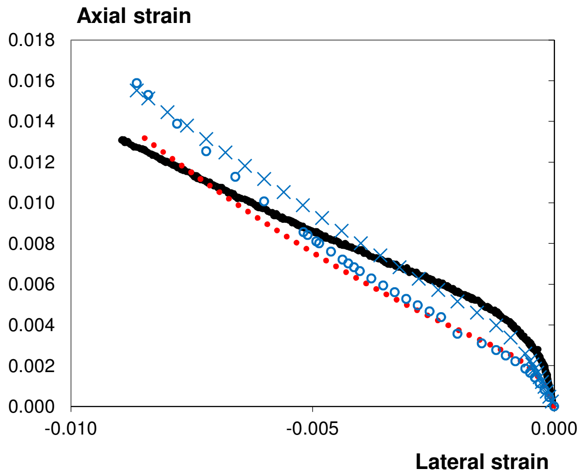

b) Axial-to-lateral strain relation

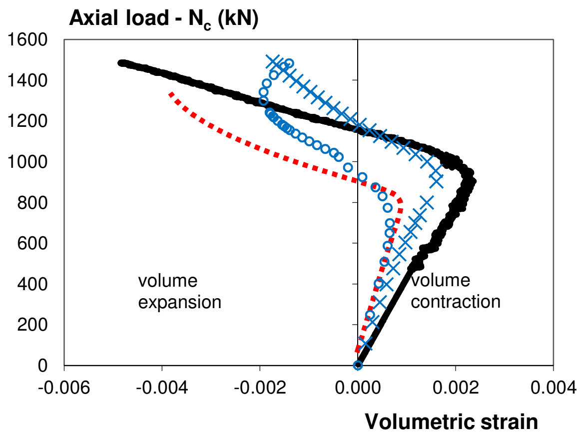

c) Axial load – volumetric load relation

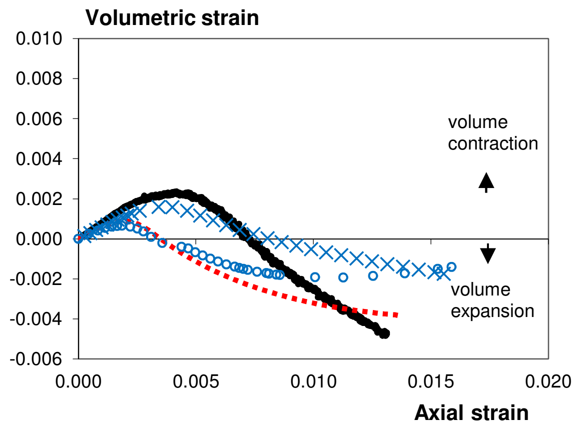

d) Volumetric strain – Axial strain relation

Fig. 13 – Test results vs Chastre and Silva (2010), Toutanji revised (2006) and Teng et al. (2007) modelling results: 150 mm diam. CFRP-confined RC column; 2 plies of t_f=0.167 mm

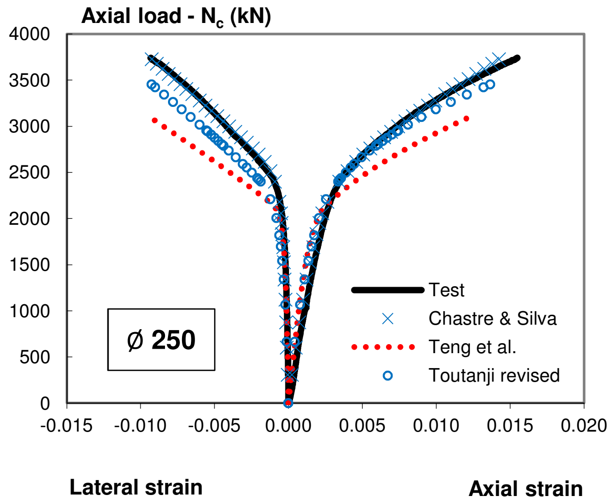

a) Axial load – lateral strain (left)
Axial load – axial strain (right)

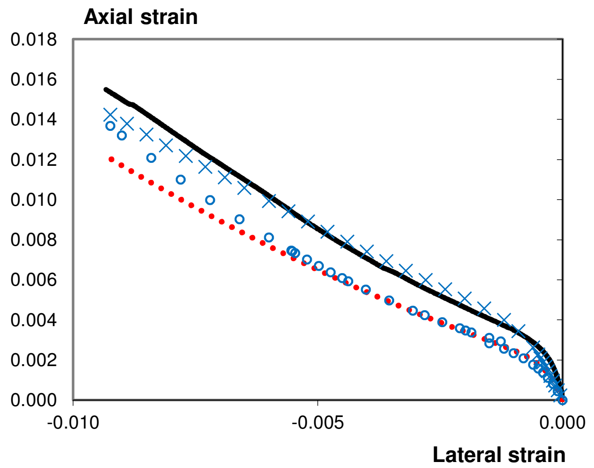

b) Axial-to-lateral strain relation

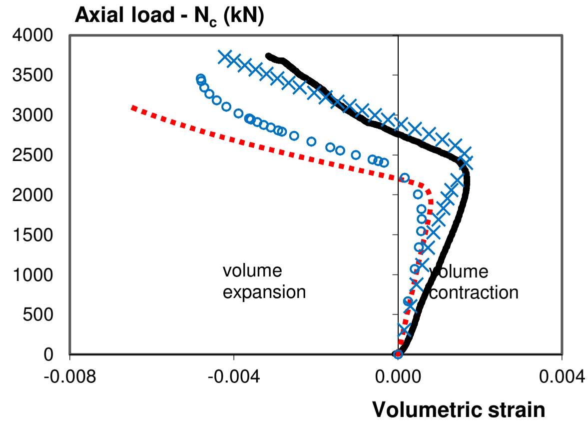

c) Axial load – volumetric load relation

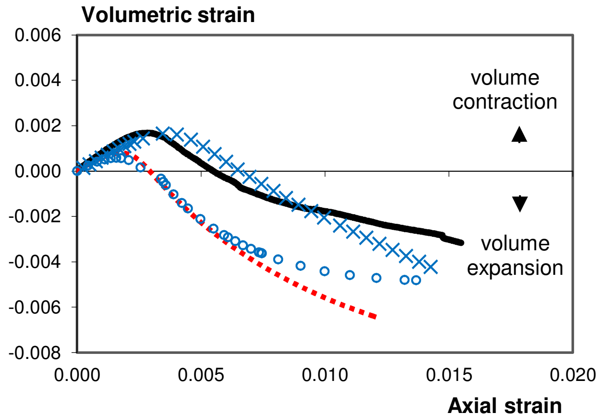

d) Volumetric strain – Axial strain relation

Fig. 14 – Test results vs Chastre and Silva (2010), Toutanji revised (2006) and Teng et al. (2007) modelling results: 250 mm diam. CFRP-confined RC column; 2 plies of t_f=0.176 mm

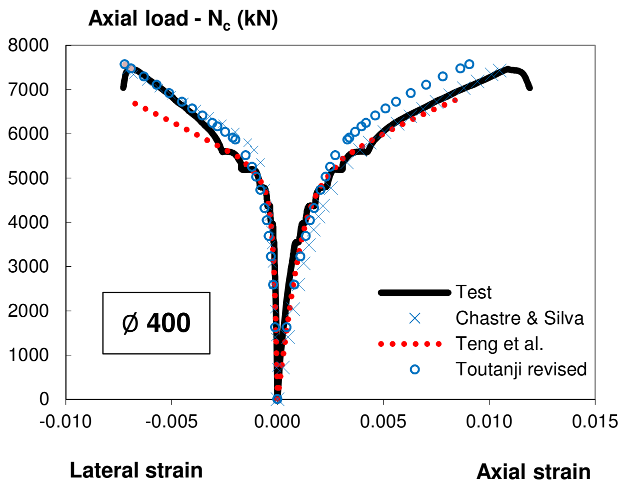

a) Axial load – lateral strain (left)
Axial load – axial strain (right)

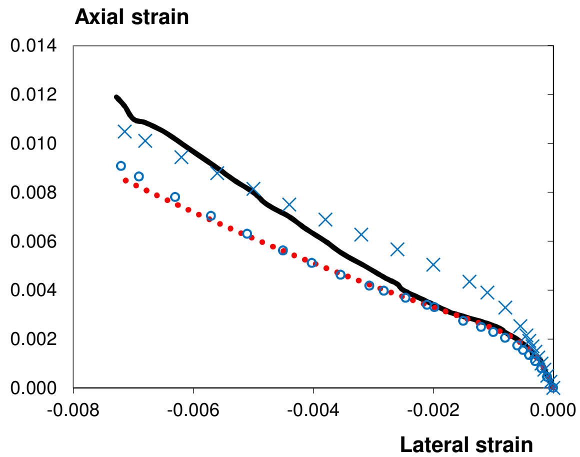

b) Axial-to-lateral strain relation

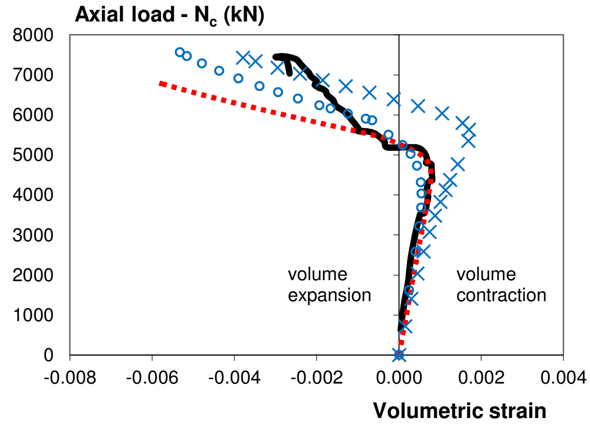

c) Axial load – volumetric load relation

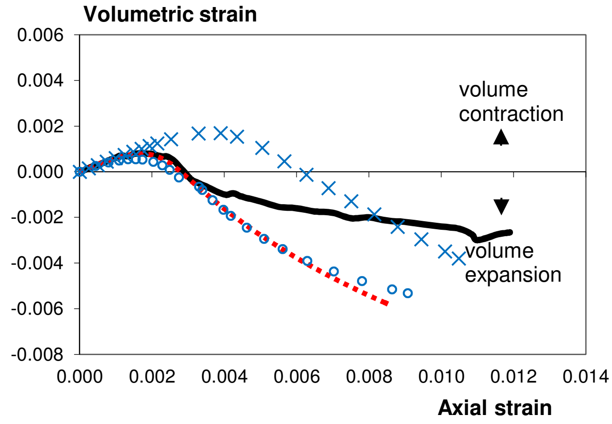

d) Volumetric strain – Axial strain relation

Fig. 15 – Test results vs Chastre and Silva (2010), Toutanji revised (2006) and Teng et al. (2007) modelling results: 400 mm diam. CFRP-confined RC column; 5 plies of t_f=0.117 mm

5. Conclusions

This article has presented the analysis of 9 confinement models for FRP-confined concrete, in view of tests results of confined concrete columns with diameters of 150, 250 and 400 mm. Four of these models are based on an analysis oriented stress-strain relation while the remaining 5 have a design oriented approach.

From the several compared parameters, the study of the load-strain relations (both axial and lateral) and the dilation behaviour, Chastre and Silva's model (2010) appears to be the most accurate predictive model among those herein studied.

The discussion of all modelling results in face of the tests results herein presented lead to the following conclusions:

- Some of the models predict accurately (say error < 10%) the peak load for the three tested diameters – Chastre and Silva (2010), Toutanji revised (2060), Samaan et al. (1998) and Saafi et al. (1999). Yet, only Chastre and Silva's model has in all three cases a load – axial strain curve shape close to tests curves in all three cases;

- For the axial strain at peak load most models give poor predictions (say error: 50% – 144%) except for: Chastre and Silva (2010) (18%, -8%, -12%), Toutanji revised (2006) (21%, -12%, 7%) and Teng et al. (2007) (3%, -22%, -29%), for the three diameters; Toutanji (1999) (27%, 1%) and Saafi et al. (1999) (31%, 7%) for 250 and 400 mm diameter, respectively;

- As to the axial-to-lateral relationship, figs 4b, 5b and 6b show that Chastre and Silva (2010) have the most accurate results for the three diameters while Toutanji revised (2006) present a close curve for the 250 mm diameter test curve, Teng et al. (2007), Toutanji (1999) and Saafi et al. (1999) present also closer curves for the 150 mm diameter test curve, although the two last authors extend their both lateral and axial strains far beyond tests limits. From this general analysis it is fair to conclude that the models that best represent the axial-to-lateral relation of confinement are those that best suit all parameters;

- The importance of the dilation behaviour on the stress-strain (load-strain) response of an FRP-confined concrete (passive confinement and linear elastic behaviour) has been proved consistent with the accuracy of results. In fact, the model that best captured the dilation behaviour – Chastre and Silva (2010) (figs. 4c, 4d, 5c, 5d, 6c and 6d) – corresponds to the one of most accurate load-axial strain curve. As exposed in section 3.4 the dilation has negligible influence on the load-lateral strain response;

- The parameters W_c, W_l and W_v, used to quantify the shape (area underneath each curve) of the several curves that express the confining behaviour of columns, are an additional useful way of assessing the performance of existing models in view of the experimental results;

- Taking into account circular cross-section RC columns from 150 to 400mm diameter confined with CFRP sheets, the several curves of results and all the presented parameters, the model with best performance among the 9 models herein studied is Chastre and Silva's (2010), although in some of the analysed parameters followed by the modelling results of Toutanji revised (Matthys et al. 2006) .Among all models, Chastre and Silva (2010) is the only that explicitly accounts for the confinement contribution given of steel hoops in the concrete columns.

The purpose of the present study is to give a contribution to the investigation on the behaviour of RC circular columns confined with CFRP since the start of compressive loading until failure. Even though several parameters such as peak load, corresponding strain and lateral failure stress were outlined and analysed, the analysis of the shape of each curve was considered of major relevance for the comparison between all models. This is why the additional parameters W_c, W_l and W_v were created, so that the shape of each modelling curve could be assessed in view of the experimental curves. It is important, however, to carry out and continue this comparative analysis with more experimental tests since the present study might be statistically limited.

References

Ahmad, S. H. and Shah, S. P. (1982). "Stress-strain curves of concrete confined by spiral reinforcement." J. Americ Concr. Inst., 79(6), 484–490.

Chastre (2005). "Comportamento às acções cíclicas de pilares de betão armado reforçados com materiais compósitos." PhD thesis, Universidade Nova de Lisboa, Lisboa.

Chastre, C. and Silva, M. A. G. (2010). "Monotonic axial behavior and modelling of RC circular columns confined with CFRP." Engineering Structures 32(8): 2268-2277.

Fam, A. Z., and Rizkalla, S. H. (2001). "Confinement model for axially loaded concrete confined by circular fiber-reinforced polymer tubes." ACI Struct. J., 98(4), 451–461.

Grassl, P. (2004). "Modelling of dilation of concrete and its effect in triaxial compression." Finite Elements in Analysis and Design 40(9-10): 1021-1033.

Howie, I. and V. M. Karbhari (1995). "Effect of Tow Sheet Composite Wrap Architecture on Strengthening of Concrete due to Confinement .1. Experimental Studies." Journal of Reinforced Plastics and Composites 14(9): 1008-1030.

Jiang, T. and J. Teng (2007). "Analysis-oriented stress–strain models for FRP–confined concrete." Engineering Structures 29(11): 2968-2986.

Karbhari, V. M., and Gao, Y. (1997). "Composite jacketed concrete under uniaxial compression—Verification of simple design equations." J. Mater. Civ. Eng., 9(4), 185–193.

Lam, L. and J. Teng (2003). "Design-oriented stress–strain model for FRP-confined concrete." Construction and Building Materials 17(6-7): 471-489.

Lee, C. and Hegemier, G.(2009). "Model of FRP-Confined Concrete Cylinders in Axial Compression." J. Comp. Constr. 13(5): 442-454.

Mander, J. B., Priestley, M. J. N., and Park, R. (1988). "Theoretical stress-strain model for confined concrete." J. Struct. Eng., 114(8), 1804–1826.

Matthys, S., Taerwe, L., and Audenaert, K. (1999). "Tests on axially loaded concrete columns confined by FRP sheet wrapping." Proc., 4th. Int. Symp. on FRP for Reinforced Concrete Structures (FRPRCS- 4), Baltimore, C. W. Dolan, S. H. Rizkalla, A. Nanni, eds., ACI SP-188, 217–228.

Matthys, S. (2000). Structural Behaviour and Design of Concrete Members Strengthened with Externally Bonded FRP Reinforcement. Department of Structural Engineering. Gent, University of Gent. Doctor of Applied Sciences, DSc.

Matthys, S., Toutanji H. and Taerwe, L. (2006). "Stress–Strain Behavior of Large-Scale Circular Columns Confined with FRP Composites." Journal of Structural Engineering 132(1).

Mirmiran, A. and M. Shahaway (1997). "Behaviour of Concrete Columns Confined by Fiber Composites." Journal of Structural Engineering 123(5).

Mirmiran, A. and M. Shahawy (1997). "Dilation characteristics of confined concrete." Mechanics of Cohesive-Frictional Materials 2(3): 237-249.

Nanni, A. and N. M. Bradford (1995). "FRP Jacketed Concrete under Uniaxial Compression." Construction and Building Materials 9(2): 115-124.

Picher, F.; Rochette, P.; and Labossiere, (1996) P., "Confinement of Concrete Cylinders with CFRP," Proceedings, 1st International Symposium on Composites for Infrastructures, H. Saadatmanesh and M. Ehsani, eds., Tucson, Ariz., pp. 829-841.

Richard, R. M. and B. J. Abbott (1975). "Versatile Elastic-Plastic Stress-Strain Formula." Journal of the Engineering Mechanics Division-Asce 101(4): 511-515.

Richart, F. E., Brandtzaeg, A., and Brown, R. L. (1928). "A study of the failure of concrete under combined compressive stresses." Bulletin No. 185, University of Illinois Engineering Experimental Station, Champaign, Ill.

Richart, F. E., Brandtzaeg, A., and Brown, R. L. (1929). "The failure of plain and spirally reinforced concrete in compression." Bulletin No. 190, University of Illinois Engineering Experimental Station, Champaign, Ill.

Saadatmanesh, H., Ehsani, M. R., and Li, M. W. (1994). "Strength and ductility of concrete columns externally reinforced with fiber composite straps." ACI Struct. J., 91(4), 434–447.

Saafi, M., Toutanji, H. A., and Li, Z. (1999). "Behavior of concrete columns confined with fiber reinforced polymer tubes." ACI Mater. J., 96(4), 500–509.

Samaan, M., A. Mirmiran, et al. (1998). "Model of concrete confined by fiber composites." Journal of Structural Engineering-ASCE 124(9): 1025-1031.

Silva, M. G.; Chastre Rodrigues, C. (2006). "Size and Relative Stiffness Effects on Compressive Failure of Concrete Columns Wrapped With GFRP." Journal of Materials in Civil Engineering, 18 (3), 334-342.

Spoelstra, M. and G. Monti (1999). "FRP-Confined Concrete Model." Journal of Composites for Construction 3(3).

Teng, J., Y. Huang, et al. (2007). "Theoretical Model for Fiber-Reinforced Polymer-Confined Concrete." Journal of Composites for Construction 11(2).

Toutanji, H. (1999), "Stress-Strain Characteristics of Concrete Columns Externally Confined with Advanced Fiber Composite Sheets," ACI Materials Journal, 96(3): 397-404.

Toutanji, H. and Y. Deng (2002). "Strength and durability performance of concrete axially loaded members confined with AFRP composite sheets." Composites Part B: engineering 33: 255-261.